

See discussions, stats, and author profiles for this publication at: <https://www.researchgate.net/publication/231436075>

DNA binding studies and site selective fluorescence sensitization of an anthryl probe. J Am Chem Soc

ARTICLE *in* JOURNAL OF THE AMERICAN CHEMICAL SOCIETY · SEPTEMBER 1993

Impact Factor: 12.11 · DOI: 10.1021/ja00072a004

CITATIONS

494

READS

38

2 AUTHORS, INCLUDING:



Challa V Kumar

University of Connecticut

186 PUBLICATIONS 5,783 CITATIONS

SEE PROFILE

DNA Binding Studies and Site Selective Fluorescence Sensitization of an Anthryl Probe

C. V. Kumar* and Emma H. Asuncion

Contribution from the Department of Chemistry, University of Connecticut, Storrs, Connecticut 06269-3060

Received March 3, 1993

Abstract: (9-Anthrylmethyl)ammonium chloride (AMAC, **1**) binds to natural and synthetic DNA sequences with a high affinity, as deduced from the absorption and fluorescence spectral data. Scatchard plots constructed from these data gave binding constants in the range $(2-8) \times 10^4 \text{ M}^{-1}$ of base pairs. Extensive hypochromism, broadening, and red shifts in the absorption spectra were observed when AMAC binds to various sequences of synthetic and natural DNA. Upon binding to DNA, the fluorescence from the anthryl chromophore was efficiently quenched by the DNA bases and the fluorescence spectra at high concentrations of CT DNA show significant broadening of the vibronic bands. Stern-Volmer quenching constants obtained from the linear quenching plots strongly depended on the DNA sequence. A high quenching constant of $1.4 \times 10^4 \text{ M}^{-1}$ for dI-dC sequences and a low value of $2.1 \times 10^3 \text{ M}^{-1}$ for homo AT sequences were estimated from this data. Time-resolved fluorescence measurements clearly show a biexponential decay behavior (lifetimes 8.2 and 30.6 ns) for AMAC bound to CT DNA. The fluorescence spectra obtained 50 ns after the excitation showed considerable red shift when compared to the spectra at early times. The red-shifted, long-lived emission spectra were consistent with the intercalative binding of **1**. Triplet-triplet absorption spectra of AMAC in the presence of CT DNA show the complete quenching of the anthryl triplet by the DNA bases. Fluorescence polarization measurements with AMAC and various DNA sequences suggest that the bound chromophore is rigid on nanosecond time scales. The melting temperatures of CT DNA and poly(dA-dT) samples were increased by AMAC binding, from 78 and 56.6 °C to 83 and 63 °C, respectively. Excitation into the absorption bands of the DNA in the 260–300-nm region, where the anthryl absorption was negligible, resulted in an intense, red-shifted, and broad fluorescence spectrum from the anthryl chromophore. The sensitized fluorescence spectra were assigned to the anthryl chromophore on the basis of the excitation spectra as well as its resemblance to the emission spectrum of the long-lived component detected in the time-resolved studies. Energy transfer from DNA bases depended on the temperature. For example, when the helix was melted, energy transfer could no longer be observed. Thus, the double-helical structure of the DNA polymer was essential for the energy transfer, consistent with the intercalative mode of binding of AMAC. It is noteworthy that binding of AMAC to DNA results in induced CD bands with distinct peaks that correspond to the absorption spectrum of the bound probe. Several pieces of strong evidence for the intercalative binding of the anthryl probe to the DNA helix are presented. The anthryl excited state serves as a sensitive probe to distinguish between homo and hetero AT sites as well as between AT and GC sites.

Introduction

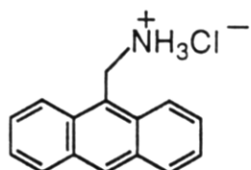
Binding studies of small molecules with deoxyribonucleic acid (DNA) are important in the design of new and more efficient drugs targeted to DNA.¹ Several aromatic hydrocarbons and their derivatives have been shown to be carcinogenic, and in several instances the carcinogenicity was attributed to their activity at the DNA level.² Metal complexes, porphyrins, natural antibiotics, and a host of other planar heterocyclic cations have been investigated for their DNA binding affinity. Recently, the DNA sequence recognition by drugs as well as by small molecules that are conjugated to peptides or oligonucleotides has been of great interest.^{3,4} Binding studies with these various small molecules are valuable for the rational design of drugs⁵ as well as in understanding how proteins recognize and bind to specific DNA sequences.⁶ Although the binding modes of several of these

molecules have been delineated, much less attention was paid to the binding of simple aromatic hydrocarbons.⁴ With a view to explore the differences in the local environment of the four DNA bases within the double helix and to exploit these differences in the design of new and more efficient DNA binding agents, we have tested the DNA binding properties of a new hydrophobic probe, (9-anthrylmethyl)ammonium chloride (AMAC, **1**) (Chart I).⁷

Poor solubility of anthracene, the parent hydrocarbon, in water prompted us to include a cationic function in the probe to improve its solubility. Cationic charge on the probe is also expected to improve the DNA binding affinity due to the increased electro-

(1) Lambert, B.; LePeco, J.-B. In *DNA-Ligand Interactions. From Drugs*

(4) Kumar, C. V.; Raphael, A. L.; Barton, J. K. *J. Biomol. Struct. Dyn.* 1986, 3, 85. Barton, J. K. *J. Biomol. Struct. Dyn.* 1983, 1, 621. Barton, J. K. *Chem. Eng. News* 1988, 66, 30. Barton, J. K. *Comments Inorg. Chem.* 1985, 3, 321. Wilson, W. D.; Wang, Y.-H.; Kusuma, S.; Chandrasekaran,

Chart I. Structure of the Anthryl Probe, AMAC

static attraction between the probe and the DNA phosphates.⁸ In general, intercalators are planar, and planarity was suggested to be one of the important features needed for efficient intercalation into the helix (Chart II).⁹ Therefore, the large planar hydrophobic anthryl moiety of the probe is expected to facilitate intercalation of the probe into the relatively nonpolar interior of the DNA helix. The methylene chain in **1** functions as a short spacer to separate the chromophore and the charge center to position the latter above or below the plane of the anthryl moiety. Thus, when the anthryl moiety intercalates into the helix, the cationic charge is positioned closer to the DNA phosphates for a favorable electrostatic interaction.

The strong absorption and fluorescence (quantum yield ~ 0.4) characteristics of the anthryl group provide a sensitive spectroscopic handle to study its interaction with DNA. The well-resolved vibronic transitions of the anthryl chromophore in the 300–400-nm region of the electronic absorption spectrum provide a spectroscopic signature for the probe environment. Changes in the intensities of these transitions can be used to decipher the nature and the strength of the stacking interactions between the chromophore and the DNA bases. Another interesting feature of the anthryl chromophore is its photochemical reactivity and its large singlet excited state energy (76 kcal/mol), which can be used to initiate photoreactions with DNA. Recently, primary alkylamines have been shown to undergo photochemical reactions with nucleotides and cause DNA strand scission.¹⁰ The primary alkylamine function present in **1** can be exploited for this purpose. Thus, AMAC has a high potential for DNA binding studies.

We have recently reported the sequence selective energy transfer from DNA bases to the anthryl chromophore in **1**.⁷ Although AMAC shows little or no sequence selectivity for binding except for homo AT sequences, highly sequence dependent energy transfer from the DNA bases to the anthryl chromophore was observed in our experiments. Energy transfer from the DNA bases to **1** was observed with AT and IC sequences, and no energy transfer was observed from GC sequences or from single-stranded nucleotides of any sequence. We now present the detailed DNA binding properties of AMAC with natural and several synthetic polynucleotides along with strong evidence for the intercalative binding of the anthryl chromophore. Intercalation of the chromophore seems to be essential for the observed sequence selective energy transfer. These observations can be exploited to initiate DNA-sensitized sequence specific photoreactions at the double helix.

Experimental Section

All DNA samples were purchased from Sigma Chemical Co. Calf thymus DNA, form I, was purified by phenol extraction, as described in the literature.¹¹ Purity of the final DNA preparation was checked by monitoring the absorption spectrum and the ratio of the absorbance at 260 to 280 nm. The synthetic deoxyribonucleotides were used as received, without further purification. All samples were dissolved in 5 mM Tris buffer, pH 7.2, 50 mM NaCl, unless mentioned otherwise. DNA concentrations per nucleotide were determined by absorption spectroscopy, using the following molar extinction coefficients ($M^{-1} \text{ cm}^{-1}$) at the

Chart II. Illustration of Ionic, Groove, and Electrostatic Binding of Small Molecules to the DNA Double Helix

indicated wavelengths: calf thymus DNA, 6600, 260 nm; poly(dA-dT), 6600, 260 nm; poly(dA)-poly(dT), 6000, 260 nm; poly(dG-dC), 8400, 254 nm; poly(dG)-poly(dC), 7400, 253 nm; and poly(dI-dC), 6900, 251 nm.¹²

(9-Anthrylmethyl)ammonium chloride (AMAC) was prepared from 9-(chloromethyl)anthracene (Lancaster) following the procedure of Bottini et al.¹³ A pale yellow solid (53% yield) was obtained, and its melting point was in agreement with the reported value.¹⁴ ¹H NMR data (Bruker 270 MHz, DMSO-*d*₆, δ 8.78 (1 H, s), 8.46 (5 H, t), 8.21 (2 H, d), 7.67 (4 H, m), 5.08 (2 H, s)), and the mass spectral peaks (EI, *m/e* (relative intensity) values 207 ($M^+ - \text{HCl}$, 79), 191 (48), 178 (65), 36 (100)) confirmed the structure of the product.

All the absorption spectra were recorded on a Perkin-Elmer Lambda 3B spectrophotometer, and all the fluorescence spectra were recorded on a Perkin-Elmer LS5B spectrometer. Both spectrometers were interfaced with an Apple Macintosh computer. All the necessary software to control the spectrometers and to analyze the data were developed in our laboratory. The absorption and the fluorescence titrations were performed by keeping the concentration of the probe constant while varying the nucleic acid concentration. This was done by dissolving an appropriate amount of the probe in the DNA stock solution and by mixing various proportions of the probe and the DNA stock solutions while maintaining the total volume of the solution constant (1 mL). This resulted in a series of solutions with varying concentrations of DNA but with a constant concentration of the probe. In fluorescence measurements, the solutions were excited at 388 nm and the fluorescence intensity was monitored at 415 nm. The intrinsic binding constant of AMAC with calf thymus DNA was determined by absorption and fluorescence titrations. In the case of the former, the absorbance at 365 nm was recorded after each addition of CT DNA. The intrinsic binding constant K was determined from the plot of $D/\Delta\epsilon_{\text{ap}}$ vs D , where D is the concentration of DNA in base pairs, $\Delta\epsilon_{\text{ap}} = [\epsilon_{\text{B}} - \epsilon_{\text{F}}]$, and $\Delta\epsilon = [\epsilon_{\text{B}} - \epsilon_{\text{F}}]$.¹⁵ The apparent extinction coefficient, ϵ_{a} , is obtained by calculating $A_{\text{obsd}}/[\text{AMAC}]$. ϵ_{B} and ϵ_{F} correspond to the extinction coefficient of the bound form of AMAC and the extinction coefficient of free AMAC, respectively. The data were fitted to eq 1, with a slope equal to $1/\Delta\epsilon$ and a y -intercept equal to $1/\Delta\epsilon K$. ϵ_{B} was determined from $\Delta\epsilon$, and K was obtained from the ratio of the slope to the y -intercept.

$$D/\Delta\epsilon_{\text{ap}} = D/\Delta\epsilon + 1/\Delta\epsilon K \quad (1)$$

In fluorescence quenching experiments, the data were plotted according to the Stern–Volmer equation (2), where I_0 and I are the fluorescence intensities in the absence and in the presence of DNA. K_{SV} is the Stern–Volmer quenching constant, which is a measure of the efficiency of quenching by DNA. Data from the fluorescence titrations were also

$$I_0/I = 1 + K_{\text{SV}}[\text{DNA}] \quad (2)$$

used to determine the binding constant of AMAC with CT DNA. The solutions were excited at 390 nm, and the probe emission was monitored at 415 nm. The concentration of the free probe was determined using eq 3,¹⁶ where C_T is the concentration of the probe added, C_F is the concentration of the free probe, and I and I_0 are the fluorescence intensities

(12) Barton, J. K.; Goldberg, J. M.; Kumar, C. V.; Turro, N. J. *J. Am. Chem. Soc.* **1986**, *108*, 2081. Baguley, B. C.; Falkenhag, E.-M. *Nucleic Acids Res.* **1978**, *5*, 161.

(13) Bottini, A. T.; Dev, V.; Klinck, J. *Organic Syntheses*; Wiley: New York, 1973; Collect. Vol. V, p 121.

(14) Stezowski, J. J.; Stigler, R.-D.; Joos-Guba, G.; Kahre, J.; Losch, G.-R.; Carrell, H. L.; Peck, R. M.; Glusker, J. P. *Cancer Res.* **1984**, *44*, 5555.

(15) (a) Pyle, A. M.; Rehmann, J. P.; Meshoyrer, R.; Kumar, C. V.; Turro, N. J.; Barton, J. K. *J. Am. Chem. Soc.* **1989**, *111*, 3051. (b) Wolfe, A.; Shimer, G. H., Jr.; Meehan, T. *Biochemistry* **1987**, *26*, 6392.

(16) Tubbs, R. K.; Dittmars, W. E., Jr.; Van Winkle, Q. J. *Mol. Biol.* **1964**, *9*, 545. Chaires, J. B.; Dattagupta, N.; Crothers, D. M. *Biochemistry* **1982**, *21*, 3933.

(8) Lavery, R.; Pullman, B. *Int. J. Quantum Chem.* **1981**, *20*, 259. Manning, G. S. *J. Chem. Phys.* **1969**, *51*, 924. Manning, G. S. *Acc. Chem. Res.* **1979**, *12*, 443. Manning, G. S. *Q. Rev. Biophys.* **1978**, *11*, 179.

(9) Lerman, L. S. *J. Mol. Biol.* **1961**, *3*, 18.

(10) Saito, I.; Sugiyama, H.; Matsuura, T. *J. Am. Chem. Soc.* **1983**, *105*, 956.

(11) Maniatis, T.; Fritsch, E. F.; Sambrook, J. *Molecular Cloning: A Laboratory Manual*; Cold Spring Harbor Laboratory: New York, 1982; p 458.

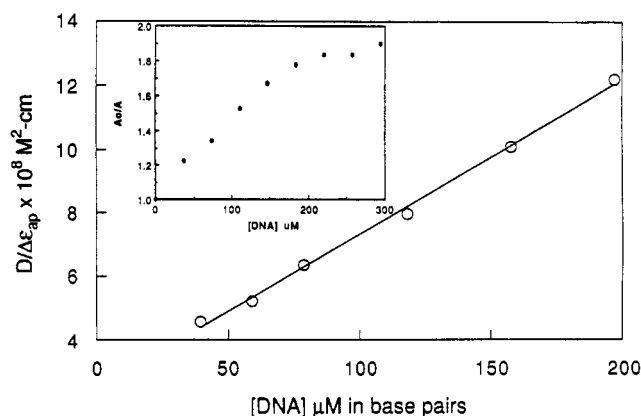


Figure 1. Half-reciprocal plot of AMAC binding with CT DNA as determined from the absorption titration data; $K = 1.5 \pm 0.5 \times 10^4 \text{ M}^{-1}$, $\epsilon_F = 3220 \text{ M}^{-1} \text{ cm}^{-1}$, $\epsilon_B = 1160 \text{ M}^{-1} \text{ cm}^{-1}$. Inset: plot of the absorption titration data at 365 nm, demonstrating the saturation of binding of AMAC to CT DNA.

in the presence and in the absence of DNA, respectively. P is the ratio

$$C_F = C_T(I/I_0 - P)/(1 - P) \quad (3)$$

of the observed fluorescence quantum yield of the bound probe to that of the free probe. The value of P was obtained from a plot of I/I_0 vs $1/[DNA]$ such that it is the limiting fluorescence yield given by the y -intercept. The amount of bound probe (C_B) at any concentration was equal to $C_T - C_F$. A plot of r/C_F vs r , where r is equal to $C_B/[DNA]$, was constructed according to the modified Scatchard equation 4 given

$$r/C_F = K_i(1 - nr)[(1 - nr)/(1 - (n - 1)r)]^{n-1} \quad (4)$$

by McGhee and von Hippel.¹⁷ In eq 4, K_i is the intrinsic binding constant and n is the binding site size in base pairs. The binding data were fitted to eq 4 with Kaleida graph software on a Macintosh computer to extract the binding parameters. The values of K_i and n were obtained from the best fit of the data to eq 4.

The DNA melting studies were done by controlling the temperature of the sample cell with a Fisher circulating bath while monitoring the absorbance at 260 nm or the fluorescence of the sample at 430 nm. The temperature of the solution was continuously monitored with a thermocouple attached to the sample holder. The absorption or the emission data were then plotted as a function of temperature.

Fluorescence lifetimes and time-resolved fluorescence spectra were obtained on a home-built single photon counting spectrometer. The excitation source was a deuterium-filled nanosecond flash lamp (F-195) from Edinburgh Instruments with a spark gap of 0.5 mm, and the full width at half-maximum of the excitation pulse was 1.6 ns. The fluorescence signal from the sample was collected with appropriate optics and passed through a monochromator (H-10, ISA Instruments, 2-mm slits), and a Hamamatsu R-955 photomultiplier was used as the detector. The single photon counting data were obtained with an EG&G multichannel analyzer card installed in an IBM PS/2 Model 30 personal computer. Software necessary for the collection and manipulation of the data was developed in our laboratory. The fluorescence decay profiles were deconvoluted with software from PRA Inc., and the goodness of fits was tested from various parameters such as χ^2 and the Durbin-Watson parameter and from the correlation function.

The fluorescence polarization measurements were carried out on a Perkin-Elmer LS-50 fluorescence spectrometer. For these measurements, the ratio of probe to DNA phosphate concentration was kept at 1:40 to ensure complete binding of the probe. The samples were excited at 388 nm, and the fluorescence signal was monitored at 415 nm, through crossed polarizers.

The circular dichroism spectra were obtained with a Jasco-710 spectropolarimeter, at room temperature. The triplet-triplet absorption spectra were recorded on a home-built flash photolysis apparatus with a gated diode array detector. A Lambda LPX-100 excimer laser (308 nm, 20 mJ per pulse, 18 ns full width at half-maximum) was used to excite the sample, and the transient species were probed with a 150-W PTI xenon lamp source. The diode array detector was gated with 10-ns

gating pulses at varying time delays after the excitation. The entire flash photolysis apparatus was interfaced with an Apple Macintosh SE computer for automated data collection.

Results and Discussion

Fluorescence and absorption properties of AMAC change dramatically as a result of binding to DNA, and these changes have been quantified to estimate binding constants and sequence specificities and to evaluate the DNA binding mode. Strong hypochromism, extensive broadening, red shift of the vibronic bands, lengthening of the excited-state lifetimes, induced circular dichroism, and increased stability of the DNA double helix were observed when AMAC binds to DNA.

Absorption Studies. The electronic absorption spectra of AMAC in the presence of increasing amounts of CT DNA showed strong decreases in the peak intensities (hypochromicity). The change in the absorbance of **1** at 365 nm with increasing concentration of calf thymus DNA (CT DNA) was used to construct the half-reciprocal plot shown in Figure 1. A continuous decrease in the intensity of AMAC absorption was followed by saturation at high concentrations of DNA (inset in Figure 1). It is important to note that the absorbance is reduced to nearly half the initial value ($\sim 50\%$ hypochromicity). The half-reciprocal plot of the absorption titration data according to eq 1 gave a linear plot and resulted in an intrinsic binding constant (K) of $1.5 \pm 0.5 \times 10^4 \text{ M}^{-1}$ in base pairs. The hypochromicity observed with AMAC (55%) was much greater than with other intercalators, reported in the literature.¹⁸ Hypochromism was suggested to be due to a strong interaction between the electronic states of the intercalating chromophore and that of the DNA bases.^{19,20} Since the strength of this electronic interaction is expected to decrease as the cube of the distance of separation between the chromophore and the DNA bases,²⁰ the observed large hypochromism strongly suggests a close proximity of the anthryl chromophore to the DNA bases. For example, intercalation of the anthryl chromophore into the helix and strong overlap of the $\pi-\pi^*$ states of the anthryl with the electronic states of the DNA bases are consistent with the observed spectral changes. In addition to the decrease in intensity, a small red shift, extensive broadening, and an isosbestic point at 388 nm were also observed in the spectra.⁷ These various spectral changes are consistent with the intercalation of AMAC into the DNA base stack.¹⁹

The extent of hypochromism observed with **1**, upon binding to DNA, was found to depend only weakly on the DNA sequence 52% (poly(dI-dC)), 55% (CT DNA), 59% (poly(dG-dC)) and was very low (14%) with the homopolymer poly(dA)-poly(dT). The narrow range of hypochromicity data with different sequences indicates the nonspecific high affinity of AMAC for all sequences of DNA. The exceptionally low value recorded for poly(dA)-poly(dT) is highly consistent with observations made with other intercalators. In general, intercalators prefer binding to alternating purine-pyrimidine sequences²¹ and, thus, the low hypochromism observed with poly(dA)-poly(dT) indicates a low affinity of AMAC for these sequences. Weak binding of **1** to this polymer is perhaps due to the large tilt of the adenine bases which participate in bifurcated hydrogen bonding with thymine residues on the opposite strand and prevent intercalation of the planar

(18) Waring, M. J. *J. Mol. Biol.* **1965**, *13*, 269.

(19) Long, E. C.; Barton, J. K. *Acc. Chem. Res.* **1990**, *23*, 271. Dougherty, G.; Prigam, W. J. *Crit. Rev. Biochem.* **1982**, *12*, 103. Berman, H. M.; Young, P. R. *Annu. Rev. Biophys. Bioeng.* **1981**, *10*, 87.

(20) Cantor, C.; Schimmel, P. R. *Biophysical Chemistry*; W. H. Freeman: San Francisco, 1980; Vol. 2, p 398.

(21) Krugh, T. R.; Reinhardt, C. G. *J. Mol. Biol.* **1975**, *97*, 133. Neidle, S. In *Progress in Medicinal Chemistry*; Ellis, G. P., West, G. B., Eds.; Elsevier: Amsterdam, 1979; Vol. 16, p 151. Wilson, W. D.; Jones, R. L. *Adv. Pharmacol. Chemother.* **1981**, *18*, 17. Waring, M. J. In *The Molecular Basis of Antibiotic Action*, 2nd ed.; Gale, E. F., Cundliffe, E., Reynolds, P. E., Richmond, M. H., Waring, M. J., Eds.; Wiley: London, 1981; p 258.

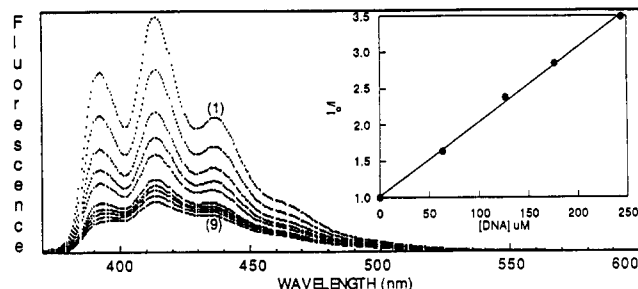


Figure 2. Fluorescence spectra of $10 \mu\text{mol dm}^{-3}$ AMAC with increasing concentration of CT DNA (0 – $370 \mu\text{mol dm}^{-3}$), with excitation at 350 nm . Inset: Stern–Volmer quenching plot of AMAC with increasing concentration of CT DNA, with excitation at 388 nm and monitoring at 415 nm .

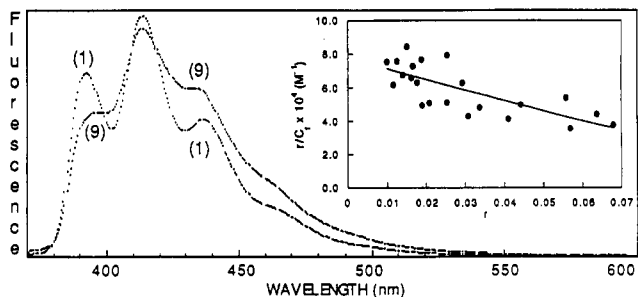


Figure 3. Normalized fluorescence spectra of $10 \mu\text{mol dm}^{-3}$ AMAC (1) in the absence and (9) in the presence of $370 \mu\text{mol dm}^{-3}$ CT DNA, with excitation at 350 nm . A broad fluorescence spectrum is observed in the presence of CT DNA. Inset: Scatchard plot of the fluorescence titration data, with excitation at 390 nm . Emission was monitored at 415 nm , $K = 7.8 \times 10^4 \text{ M}^{-1}$, $n = 4.8$ in base pairs.

moiety into the helix.²² It is noteworthy that neither broadening nor hypochromism of the absorption spectra was observed when **1** binds to a polyanion such as poly(sodium 4-styrenesulfonate) or to sodium dodecyl sulfate micelles.²³ Thus, the absorption spectral changes observed with DNA are unique and are not due to mere electrostatic binding of the cations to the DNA phosphate backbone. The narrow range of hypochromism values observed with several different synthetic DNAs emphasizes the nonpreferential binding of the anthryl probe to AT as well as GC sequences with the exception of homo AT sequences.

Fluorescence Studies. Binding of the anthryl probe to the DNA helix was found to quench the probe fluorescence very strongly. Thus, the fluorescence intensity of **1** decreases rapidly with increasing concentration of CT DNA (Figure 2 and the inset). The fluorescence quenching constant evaluated using the Stern–Volmer equation (2) was $1 \times 10^4 \text{ M}^{-1}$ of DNA phosphates. It is clear that quenching was not saturated even at high concentrations of DNA, and time-resolved fluorescence studies show that quenching by DNA is essentially static. Lack of saturation in the quenching plot even when the binding is saturated indicates that only a fraction of the binding sites quench the fluorescence. Close examination of the fluorescence spectra in the presence of large amounts of CT DNA (Figure 3) shows small, but reproducible, changes in the relative intensities of various vibrational bands. The spectra at high DNA concentrations were also considerably broad due to the superposition of spectra from bound and free chromophores which are shifted in wavelength with respect to each other.

(22) Wang, A. H. J.; Teng, M.-K. In *Crystallographic and Modeling Methods in Molecular Design*; Bugg, C. E., Ealick, S. E., Eds.; Springer-Verlag: New York, 1990; p 123. Teng, M. K.; Fredrick, C. A.; Usman, N.; Wang, A. H. *Nucleic Acids Res.* **1988**, *16*, 2671–2690.

(23) Absorption and fluorescence titrations with a polyanion such as poly(sodium 4-styrenesulfonate) or with anionic micelles of sodium dodecyl sulfate did not show the changes observed with DNA, unpublished results.

Table I. K_{SV} Values for AMAC Fluorescence Quenching by Various DNA Sequences

DNA	$K_{SV}^a (\text{M}^{-1})$	DNA	$K_{SV}^a (\text{M}^{-1})$
poly(dI-dC)	1.4×10^4	calf thymus DNA	1.0×10^4
poly(dG-dC)	1.2×10^4	poly(dA-dT)	7.4×10^3
		poly(dA)-poly(dT)	2.1×10^3

^a The estimated error in the K_{SV} values was $\pm 5\%$.

Scatchard Analysis of the Fluorescence Data. The fluorescence titration data were analyzed to construct the binding isotherms, and from these isotherms, binding constants as well as binding site sizes were estimated. A plot of r/C_F vs r gave the binding isotherm, and best fit of the data to eq 4 resulted in a binding constant of $7.8 \times 10^4 \text{ M}^{-1}$ of base pairs and a site size of 4.8 ± 1 base pairs (inset, Figure 3). On the other hand, the absorption titration data gave an intrinsic binding constant (K) of $2.0 \times 10^4 \text{ M}^{-1}$, and the estimated value of ϵ_B was $1160 \text{ M}^{-1} \text{ cm}^{-1}$, from these data. The binding constants obtained from the two methods are consistent, within the experimental error of the two different methods, and lend credibility to these measurements. The large binding constant observed for AMAC is indicative of the high affinity of the anthryl chromophore for the DNA base pairs. The estimated site size of ~ 4 base pairs for this aromatic cationic probe is consistent with the neighbor exclusion model for the intercalation of **1** into the helix, and our binding parameters are comparable to the values reported for typical intercalators such as ethidium and proflavin.²⁴

Sequence Dependence of Fluorescence Quenching. Quenching of probe fluorescence by DNA strongly depended upon the DNA sequence (Table I), and the order of quenching was $d(\text{IC}) > d(\text{GC}) > \text{calf thymus} \gg d(\text{AT}) \gg d(\text{A})-d(\text{T})$. Thus, GC sequences quench the fluorescence more strongly than AT sequences and the lowest quenching efficiency was observed with homo AT sequences, consistent with a low affinity of AMAC for this homopolymer. Binding affinity alone cannot account for the observed sequence dependence of the fluorescence quenching. Time-resolved fluorescence studies described later indicate that quenching observed in the steady-state experiments is entirely static. Therefore, it is likely that the extent of quenching depends upon the chemical nature of the nucleotides and binding affinity as well as the binding mode. When **1** binds to poly(sodium 4-styrenesulfonate) or to sodium dodecyl sulfate micelles, its fluorescence is not quenched. On the contrary fluorescence from **1** increases upon binding to these anionic media.²³ Thus, quenching is not due to counterion condensation or self-quenching at the negatively charged surfaces of the DNA helix. The strong dependence of quenching constants on the DNA sequence suggests that quenching is perhaps due to the intercalation of **1** into the DNA bases and not due to mere binding to the phosphate backbone. Since singlet energies of the DNA bases are greater than that of anthracene by at least 15 kcal/mol ,²⁵ the fluorescence quenching of anthryl fluorescence by DNA bases via energy transfer will be considerably uphill and unlikely.

Further insight into the fluorescence quenching mechanism was obtained from flash photolysis experiments. If the fluorescence quenching by DNA leads to enhanced intersystem crossing, then increased triplet yields are to be expected under these conditions. Intense triplet–triplet absorption spectra with a sharp peak around 440 nm , characteristic of the anthracene triplet in water, were observed when solutions of AMAC were excited by 308-nm laser radiation, from an excimer laser (supplementary material). The spectra were recorded 100 ns after the excitation pulse, with a gated optical multichannel analyzer. The triplet–triplet absorption spectrum disappeared completely in the presence of CT DNA (probe to DNA-P ratio of $1:20$). Efficient quenching of the triplet in the presence of DNA indicates either that the

(24) Schmechel, D. E. V.; Crothers, D. M. *Biopolymers* **1971**, *10*, 465. LePecq, J.-B.; Paoletti, C. *J. Mol. Biol.* **1967**, *27*, 87.

(25) Eisinger, J. *Photochem. Photobiol.* **1968**, *7*, 597–612.

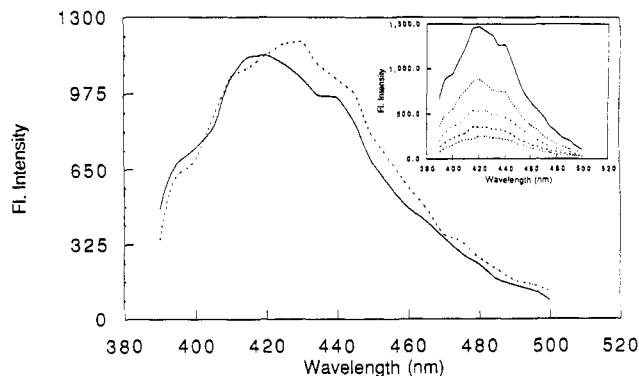


Figure 4. Normalized time-resolved emission spectra of $15 \mu\text{mol dm}^{-3}$ AMAC in the presence of $300 \mu\text{mol dm}^{-3}$ CT DNA after 15 ns (solid line) and after 53 ns (dashed line). A 15-nm shift in the fluorescence spectrum is observed, characteristic of the bound chromophore. Inset: a decrease in the fluorescence intensity, observed as a function of time.

singlet excited state is quenched directly to form the ground state without the intervention of the triplet or that the triplet is quenched faster than it is produced. In either case, the DNA quenching events are extremely fast and do not involve diffusion of the anthryl chromophore, strongly suggesting intercalation of **1** into the helix.

Time-Resolved Fluorescence Studies. Fluorescence from the free and the bound chromophore can be time-resolved if the fluorescence lifetimes of the two forms differ on the experimental time scale. If the probe is intercalated into the helix, then one expects a long-lived, red-shifted fluorescence in the presence of DNA. Although the majority of the excited states produced at the helix are quenched by the DNA bases, broadened, red-shifted fluorescence can be observed from the bound probe (Figure 4). The fluorescence decay profiles of **1**, recorded on a time-correlated single photon counting spectrometer, show a distinct biexponential behavior in the presence of CT DNA (supplementary material). Deconvolution of the decay traces using a biexponential decay law resulted in lifetimes of 8.2 and 30.6 ns for the short- and long-lived components, respectively. These values are to be compared with the single-exponential decay observed for AMAC in the absence of DNA, with a lifetime of 8.6 ns. Thus, the short-lived component measured in the presence of DNA can be assigned to the free probe and the longer-lived component to the intercalated chromophore. Such lengthening of the fluorescence lifetimes by nearly a factor of 3 constitutes strong evidence for the intercalation of the fluorophore, as reported in the literature.^{4,12,15a}

The fluorescence decay traces obtained at different emission wavelengths in the time-resolved experiments can be used to construct fluorescence spectra at various delay times following the excitation pulse (Figure 4 and the inset). The data were collected at 5-nm intervals and over a total time window of 100 ns. The spectra recorded with delay times <15 ns after the excitation pulse show one broad peak at 415 nm with two shoulders, corresponding to the spectrum of the free chromophore in the absence of DNA, recorded under the same experimental conditions. However, the spectra obtained with delay times >50 ns show considerably red-shifted emission spectra with a maximum at 430 nm (Figure 4). Such red-shifted emission spectra were indeed observed with several typical intercalators in the presence of DNA.^{4,12,15a} Red-shifted emission and the lengthened lifetimes clearly indicate the rigid, altered environment of the anthryl chromophore. Thus, the time-resolved emission studies clearly support at least two distinct chromophores in the presence of DNA, and the long-lived, red-shifted component is consistent with intercalation of AMAC into the DNA double helix.

Fluorescence Polarization Measurements. When the anthryl chromophore intercalates into the helix, its rotational motion should be restricted and, hence, fluorescence from the bound chromophore should be polarized. In the absence of DNA, fluorescence from the anthryl chromophore was weakly polarized

Table II. Polarization Values for AMAC Fluorescence in the Presence of Various DNA Sequences

DNA	polarization	DNA	polarization
AMAC, no DNA	0.008 ± 0.002	poly(dI-dC)	0.016 ± 0.001
poly(dG-dC)	0.004 ± 0.002	calf thymus DNA	0.016 ± 0.002
poly(dA)-poly(dT)	0.005 ± 0.002	poly(dA-dT)	0.018 ± 0.002

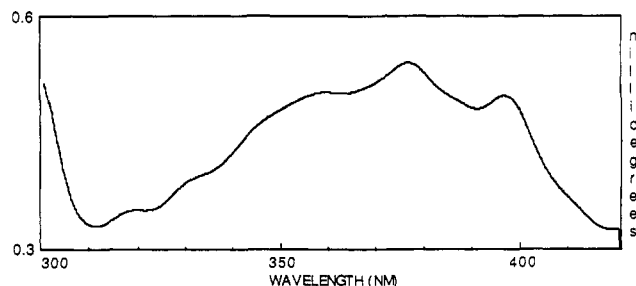


Figure 5. CD spectrum of a 1:2 AMAC to CT DNA ratio. A positive induced CD spectrum is observed, which is similar to the bound absorption spectrum.

(0.008 ± 0.002 , Table II) due to the rapid tumbling motion of the anthryl chromophore in aqueous media. However, when **1** binds to DNA containing alternating AT sequences, the fluorescence is significantly polarized (0.018 ± 0.002). The large increase in the polarization upon binding to alternating AT sequences suggests intercalation of **1** into the helix. Similarly, large polarization values were obtained with IC sequences as well (Table II). However, with poly(dG-dC) or with poly(dA)-poly(dT), the emission was not polarized (0.005 ± 0.002). Poor intercalation of AMAC to the homo AT sequences is consistent with the absence of polarized emission, and this synthetic DNA serves as an excellent control in our experiments to demonstrate that mere binding to the phosphate backbone or to the DNA grooves does not result in enhanced fluorescence polarization.

Induced Circular Dichroism Spectra. Other evidence for the strong interaction of probes with the asymmetric environment of the DNA helix comes from circular dichroism studies.²⁶ In general, intercalators bound to the helix exhibit induced circular dichroism (CD) spectra due to their asymmetric environment. The sign and magnitude of the induced CD band can be used to deduce the relative orientation of the chromophore with respect to the base pair.²⁶ Therefore, intercalation of the anthryl moiety was expected to result in CD bands in the 300–400-nm region of the spectrum, where the bound probe absorbs. The induced CD spectrum of **1** recorded in the presence of calf thymus DNA is shown in Figure 5 and displays distinct, strong positive CD bands. Such CD bands were not observed with the free probe, in the absence of DNA. It is noteworthy that the induced CD peaks correspond to the absorption bands of the bound anthryl chromophore and not the free probe, consistent with the conclusion that the induced CD bands are due to the bound AMAC and very likely from the intercalated chromophore.

DNA Melting Experiments. Other strong evidence for the intercalation of AMAC into the helix was obtained from the DNA melting studies. Intercalation of small molecules into the double helix is known to increase the helix melting temperature, the temperature at which the double helix denatures into single-stranded DNA.²⁷ The extinction coefficient of DNA bases at 260 nm in the double-helical form is much less than in the single-stranded form; hence, melting of the helix leads to an increase

(26) Lyng, R.; Hard, T.; Norden, B. *Biopolymers* **1987**, *26*, 1327. Norden, B.; Tjerner, F. *Biopolymers* **1982**, *21*, 1713. Schipper, P. E.; Norden, B.; Tjerner, F. *Chem. Phys. Lett.* **1980**, *70*, 17.

(27) Patel, D. J. *Acc. Chem. Res.* **1979**, *12*, 118. Patel, D. J.; Canuel, L. L. *Proc. Natl. Acad. Sci. U.S.A.* **1976**, *73*, 3343. Berman, H. M.; Young, P. B. *Annu. Rev. Biophys. Bioeng.* **1981**, *10*, 87.

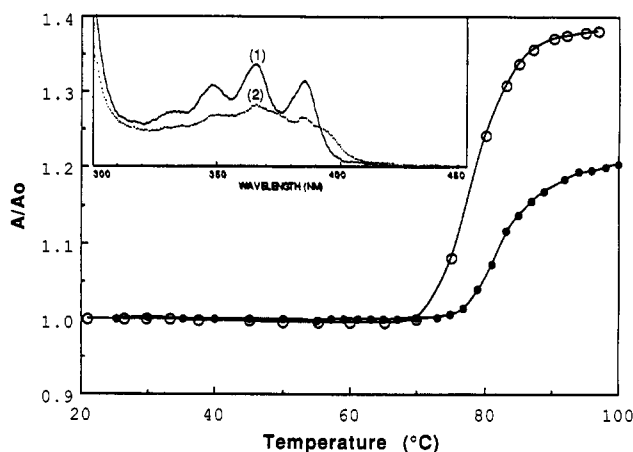


Figure 6. Plots of A/A_0 vs temperature of $160 \mu\text{mol dm}^{-3}$ CT DNA (open circles) and CT DNA in the presence of AMAC (filled circles) with a 1:1 ratio of DNA-P to AMAC. Inset: absorption spectra of $7.2 \mu\text{mol dm}^{-3}$ AMAC in the presence of $168 \mu\text{mol dm}^{-3}$ CT DNA at (1) 90 and (2) 20 °C.

in the absorption²⁸ at this wavelength. Thus, the helix to coil transition temperature can be determined by monitoring the absorbance of the DNA bases at 260 nm as a function of temperature. The DNA melting curves in the absence and in the presence of **1** are presented in Figure 6, in the presence of 50 mM NaCl and $160 \mu\text{M}$ DNA-P. The melting temperature (T_m) of CT DNA was increased from 78 °C (in the absence of **1**) to 83 °C in the presence of **1** (1:1 ratio of DNA-P to AMAC concentration). When the NaCl concentration was reduced to 10 mM, the melting temperatures with and without the probe were 80 and 71 °C, respectively. In a separate set of experiments, we found that binding of AMAC to alternating AT sequences also increases the melting temperature from 56.6 to 63 °C. These large increases in the helix melting temperatures in the presence of **1**, at two different salt concentrations, clearly establish the increased stability of the double helix when **1** binds to DNA. These increases in the melting temperatures are comparable to the values observed with the classical intercalator ethidium and lend strong support for the intercalation of **1** into the helix.²⁷

When the double helix is denatured, the AMAC absorption spectrum sharpens and returns to the shape and intensity of the free probe (spectrum 1, inset in Figure 6), indicating that the broad and red-shifted absorption spectrum of AMAC in the presence of CT DNA (spectrum 2, inset in Figure 6) is due to intercalation into the double helix and not to binding to the single-stranded DNA or to the phosphate backbone. These results also establish that the spectral changes that accompany binding of **1** to DNA are reversible and that the anthryl chromophore was not destroyed or chemically altered in the binding process. These various DNA melting experiments clearly support intercalation of the probe into the double-helical DNA.

Fluorescence Sensitization by DNA Bases. Another interesting and unique property of AMAC binding to DNA was that the probe fluorescence can be sensitized by DNA bases.⁷ Energy transfer from the DNA bases to the anthryl chromophore was established by monitoring the fluorescence from the anthryl at 438 nm while exciting the sample at various wavelengths. In the absence of DNA, the excitation spectrum of **1** matched that of the free probe absorption spectrum. However, the excitation spectrum of the probe in the presence of CT DNA showed a new band in the 260–300-nm region, not present in the AMAC absorption spectrum. Double-helical DNA has a characteristic absorption in this region, and light absorption by DNA resulted in fluorescence from the anthryl chromophore. In control experiments, pure DNA solutions showed no excitation bands in the 250–400-nm region when monitored at 438 nm.

(28) Zubay, G. L. *Biochemistry*, 2nd ed.; Macmillan: New York, 1988; pp 236–238. Lehninger, A. L. *Biochemistry*, 2nd ed.; Worth Publishers: New York, 1975; pp 873–875.

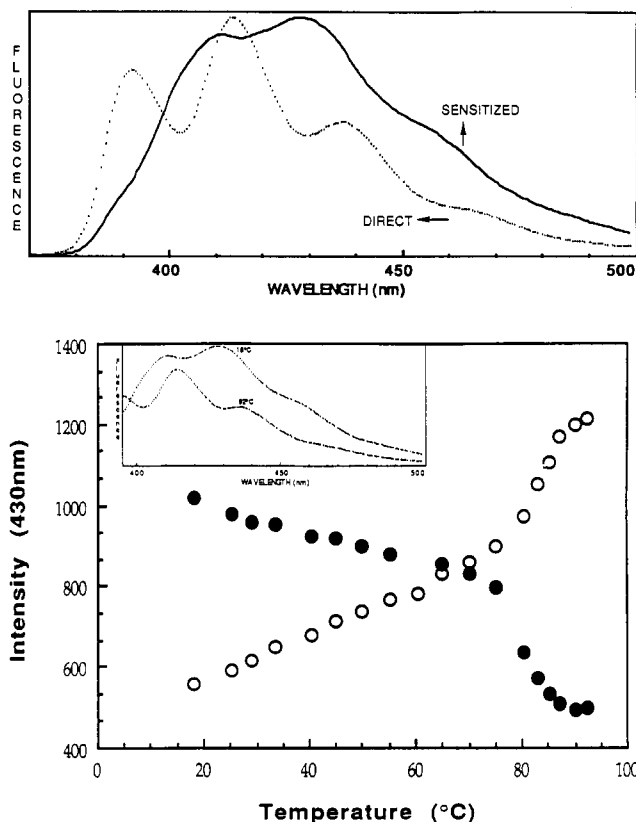


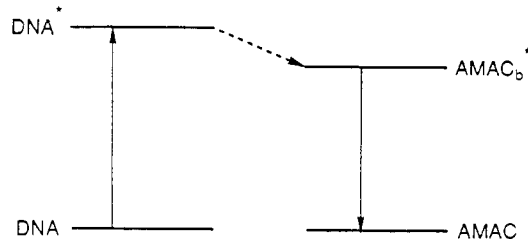
Figure 7. (A, top) Emission spectrum of free AMAC (dots, excitation at 350 nm) and the sensitized emission spectrum of AMAC in the presence of CT DNA (line, excitation at 260 nm, ratio of AMAC to DNA-P was 1:40). (B, bottom) AMAC Fluorescence intensity at 430 nm as a function of temperature in the presence of CT DNA (same concentrations). The samples were excited at 388 nm (open circles) and at 260 nm (filled circles). Inset: fluorescence spectra of $7 \mu\text{mol dm}^{-3}$ AMAC in the presence of $187 \mu\text{mol dm}^{-3}$ CT DNA at 18 and 92 °C.

Singlet-singlet energy transfer from DNA bases to the anthryl chromophore was probed by examining the fluorescence spectra while exciting into the DNA absorption bands (Figure 7A). Excitation at 260 nm of a 1:30 mixture of AMAC and CT DNA, when >99% of light was absorbed by DNA, resulted in a red-shifted, extensively broadened fluorescence spectrum with maxima at 411, 428, and 457 nm. However, the fluorescence spectrum strongly resembles that of AMAC but red shifted by nearly 20 nm, and this observation clearly establishes energy transfer from the DNA bases to the anthryl chromophore. Such large red shifts cannot be justified by simple groove binding or ionic binding of the chromophore to the DNA helix. Large red shifts and broadening of the emission spectra were also observed when ethidium and proflavin intercalate into the helix.²⁹ It is noteworthy that the sensitized emission spectrum shown in Figure 7A is quite similar to the fluorescence spectrum of the long-lived component monitored in the time-resolved studies (Figure 4).

Sensitization of the anthryl fluorescence by the DNA bases, reported above, turns out to be one of the unique features of the anthryl probe (Scheme I). The singlet excited state energies of all the four DNA bases are much higher²⁵ than that of anthracene (76 kcal/mol);³⁰ hence, singlet energy transfer from the bases to the anthryl group should be exothermic. Energy transfer from the DNA bases was also observed with several other derivatives of anthracene, such as (9,10-anthracenediyl)dimethylammonium chloride, (3-(9-anthryl)propyl)ammonium chloride, and ethyl(9-anthrylmethyl)ammonium chloride, establishing the generality of the above observation. Energy transfer from DNA to pyrene

(29) LePecq, J.-B.; Paoletti, C. C. R. *Hebd. Seances Acad. Sci.* **1964**, 259, 1786.

(30) Wilkinson, F. In *Organic Molecular Photophysics*; Birks, J. B., Ed.; Wiley: New York, 1975; p 95.

Scheme I. Energy-Transfer Scheme for the Sensitization of AMAC Emission by the DNA bases

^a Singlet energies of all four bases are higher than the anthryl singlet excited state.

or to perylene chromophores was not observed, although energy transfer to these chromophores is also expected to be exothermic. Thus, energy transfer from the DNA bases to the anthryl chromophore perhaps depends upon several factors in addition to the energies of the states involved.

The importance of intercalation into the DNA double helix in the sensitization mechanism was established in DNA melting studies. The intensity of sensitized emission from **1** was monitored as a function of temperature at a probe to DNA-P concentration ratio of 1:26, with excitation into the DNA absorption bands at 260 nm (Figure 7B). The sensitized emission intensity plotted as a function of temperature showed a strong transition around the melting temperature of CT DNA with a rapid decrease in the intensity of the sensitized emission as the helix was melted. The emission spectra obtained before and after melting of the helix (260-nm excitation) were very distinct (inset, Figure 7B). It is clear that the broad, red-shifted emission of the bound probe observed at room temperature is replaced by the fluorescence spectrum of the free probe when the helix melts. Thus, binding and intercalation into the double helix are essential for the energy transfer from the DNA to the anthryl probe. While the intensity of the sensitized emission decreases as the helix melts, the intensity of the direct emission increases (Figure 7B). Since binding of **1** to single-stranded DNA is weak, melting of the helix releases the probe into the solution and, hence, the fluorescence intensity increases as the helix melts. These various spectral results coupled with the melting studies clearly establish that the double-helical structure of the DNA is essential for the observed energy transfer from the nucleotides to the anthryl chromophore, and intercalation of the probe is highly consistent with these observations.

Sequence Dependence of Energy Transfer. Energy transfer from DNA sequences to the anthryl chromophore was shown to be highly sequence dependent, and no energy transfer was observed from alternating or homo GC sequences.⁷ The relative energy transfer efficiencies for different DNA sequences can be estimated by recording the excitation spectra at a constant ratio of probe to DNA-P concentrations, in the presence of various DNA sequences. In a plot of the ratio of the intensity observed in the presence of various DNA samples to that of the free AMAC ($I_{\text{sen}}/I_{\text{AMAC}}$), a clear peak was observed around 285 nm, in the presence of AT, IC sequences and CT DNA (Figure 8). The value of this ratio was constant and less than 1 when the experiment

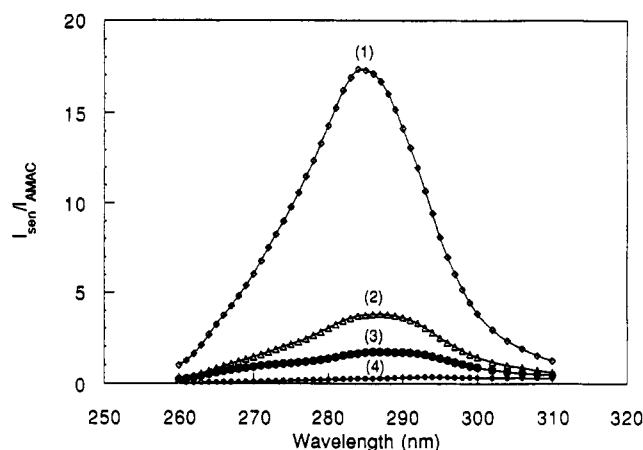


Figure 8. Ratio of the fluorescence intensity of AMAC in the presence of (1) poly(dA-dT), open diamonds, (2) CT DNA, open triangles, (3) poly(dI-dC), filled circles, and (4) poly(dG-dC), open circles, to the fluorescence intensity of AMAC in the absence of DNA at 260–310 nm. No energy transfer was observed with poly(dG-dC).

DNA to AMAC indicates that the anthryl moiety can be useful in the design of photoactivated sequence specific DNA cleavage reagents.

Conclusions

AMAC binds to the DNA double helix with binding constants on the order of 10^4 M^{-1} in DNA base pairs. Strong hypochromism (>50%) and red-shifted absorption spectra strongly support intercalation of the chromophore. Time-resolved fluorescence studies clearly indicate very long-lived fluorescence (half-life ~30 ns) that is also red shifted with respect to the free probe. From a variety of spectroscopic experiments and the DNA melting experiments, it is concluded that the anthryl chromophore intercalates into the helix. This conclusion is further reinforced by the observation that **1** shows poor affinity for homo AT sequences while showing high affinity for hetero AT sequences. Groove binders such as netropsin cannot distinguish between homo and hetero AT sequences, whereas intercalators can. The poor binding of intercalators to homo AT sites was well established, and it was suggested to be due to the large base tilt observed with these sequences, which can disfavor the insertion of a flat intercalator into the helix stack. We confirm the highly sequence dependent energy transfer from the AT bases to AMAC, which was suggested to require intercalative binding of the probe. Several other probes with the anthryl chromophore also show the sequence dependent energy transfer from the DNA bases and establish the generality of the energy-transfer process. The strong dependence of the energy transfer on the DNA sequence may be exploited in future studies for site dependent photochemistry at the DNA helix. Current results clearly indicate that it is possible to design molecular systems based on the anthryl chromophore that can bind to DNA avidly and serve as excellent model systems to